Silicon (2022) 14:1497–1510
https://doi.org/10.1007/s12633-021-00948-1

ORIGINAL PAPER

Model Prediction and Experimental Study of Material Removal Rate in Micro ECDM Process on Borosilicate Glass

Lijo Paul [1] · Somashekhar S. Hiremath [2]

Received: 6 June 2020 / Accepted: 6 January 2021 / Published online: 29 January 2021

Abstract
Miniaturization of products has become a major technological challenge in production industries. Material removal in microscopic and sub-microscopic level has become a demand for producing such products. Electro-Chemical Discharge Machining (ECDM) is one of the hybrid non-conventional machining processes to machine materials that are electrically conductive and non-conductive at a micro-level utilizing the principles of Electro Discharge Machining (EDM) and Electro-Chemical Machining (ECM). The most common nonconductive materials machined with this process are various types of glasses, ceramics, composites, etc. In the current paper, a Finite Element Model (FEM) of the ECDM process is carried out in the discharge regime (less than 300 μm) with pulsed DC in a 2D domain to characterize the Material Removal Rate (MRR) as a process output response in borosilcate glass machining. From the model and experiements the value of MRR is found to be 0.373 mg/ min and 0.414 mg/ min. It can be considered that there is almost negligible difference in MRR between experimental and model values with 9.9% error variation. Hence the results are validated with experimentation, and there is a good agreement observed between the results.

Keywords Electrochemical discharge machining · Finite element model · Material removal rate · Pulsed direct current

1 Introduction

Presently the customer requirement on the products/processes are stringent, such as extraordinary properties of materials, complex 3-D geometries, miniature features, nano-level surface finish, multifunctional properties with simple easy of operations, and low cost. Competition exists worldwide to meet the customer requirement efficiently and effectively in the stipulated period. Many engineering materials are developed to meet the customer requirements with high standards, but machining of these materials is difficult and even impossible with conventional machining processes. Borosilicate glass is one such material which have wide application in fabrication of micro structures, micro fluidic devices, MEMS and optical devices. Machining of borosilicate glass is challenging in micro domain due to its brittleness and hardness. Even if possible, with NC/CNC/DNC, there are thousands of slide movements, high MRR, high feed rates and high speed of operations required to machine 3-D geometries with required accuracies. The alternative is to develop advanced manufacturing processes in general and advanced machining processes in particular. Many new machining processes like Electro Discharge Machining(EDM), Water Jet Machining (WJM), Electro-Chemical Machining (ECM), Laser Beam Machining (LBM)...etc. has emerged as a result of these trends which can meet this demand to some extent. It is further improved by combining some of this process to produce products that meet customer demands. EDM and ECM have supported the machining of conducting materials to the required precision. Electrochemical Discharge Machining (ECDM) has emerged as a potential hybrid machining process, combining the principles of EDM and ECM to machine non-conducting materials in a highly precise manner. Many non-conventional machining process such as Chemical Etching, Abrasive Jet Machining, Laser machining have shown potential to machine borosilcate glass. Also hybrid machining process, Electro Chemical Discharge Machining (ECDM) has shown tremendous progress in effectively machining borosilcate glass. Current research work concentrate on the modelling and experimental verification of borosilicate glass

✉ Lijo Paul
lijo.paul@gmail.com

[1] Department of Mechanical Engineering, SJCET Palai, Kottayam, Kerala 686579, India

[2] Department of Mechanical Engineering, IIT Madras, Chennai, India

machining with ECDM process. Many researchers have explored many underlining principles of this hybrid machining process, theoretically and experimentally.

Kulkarni et al. [1] demonstrated the underlying mechanism of ECDM through experimental observations of varying current with time-in the circuit. They have reported the mechanism of temperature rise and Material Removal Rate (MRR) in ECDM. Fascio et al. [2] studied the variation in voltage and current characteristics while machining the glass materials using the ECDM process. A thermo physical model of ECDM was propped by Ali and Mohammed [3] using Finite Element Method (FEM) for MRR. They have found consistency in the proposed model and experimental results. Ali and Mohammed [4] have also studied the tool wear with different tools in the ECDM process and have suggested that tool life can be improved with pulse voltage in machining. Basak and Ghosh [5] introduced a theoretical model by which they demonstrated the mechanism of spark generation in ECDM. They had reported the discharge as a switching-off process in an electrical circuit. Basak and Ghosh [6] also demonstrated a method to enhance the machining process by controlling the inductance of the circuit as a process parameter. Wang et al. [7] has carried out an innovative method of combining wire electrolytic-spark slicing with electric discharge and the anodic etching process. They demonstrated high machining efficiency by combining the various process parameters and reported that the hybrid process of spark with erosion could machine and texture silicon wafer simultaneously, thereby reducing the cost of production. Jui et al. [8] have demonstrated the potential of ECDM for deep hole machining using in house developed tools and optimized process parameters. They have proved high aspect ratio machining in glass by reducing the electrolyte concentration with specially developed tools.

Pankaj et al. [9] has studied the effect of pulse duration in quality characteristics of the ECDM process and have reported that the effective range of pulse duration will improve the quality of the machined surface. Ranganayakulu et al. [10] has developed a new design for the ECDM setup. The Artificial Neuro-Fuzzy Inference System (ANFIS) has been used for modeling and reported that voltage has a predominant effect on MRR. But the predicted model only gave a comparative range for MRR in the ECDM process. Roth et al. [11] has modeled ECDM with a single spark with COMSOL software and reported that the simulation of the diameter of the heat-affected zone was less dependent on discharge duration and heat transfer due to heat flux. Paul et al. [12] has carried out non-parametric modeling of the ECDM process with Response Surface Modelling (RSM) and showed the effect of various process parameters like voltage, concentration, and duty factor on MRR. The limitation of RSM process is that the results give the trend of MRR in terms of parameter variation and do not specifically gives any numerical values of parameter combination. S. Saranya and A. R Sankar [13] have carried out a constant velocity feed method on the ECDM process on quartz substrates. They have found cylindrical tools are giving better accuracy. They have reported that precise accuracy and aspect ratio can be obtained for spherical tool electrodes with a reduction in overcuts. N.Sabahi et al. [14] machined micro channels with ECDM and studied the effect of Heat Affected Zone (HAZ) with a nano-indentation test. They have reported that HAZ got reduced to a greater extent in the presence of a magnetic field during machining. M Goud and A K Sharma [15] have used Grey Relational Approach (GRA) to find the best parameter combination in the ECDM process with MRR and Radial Over Cut (ROC) as outputs. The experimental results are verified with GRA. W.Tang et al. [16] have investigated the gas film formation in the ECDM process with high-speed imaging technology. They have reported that bubble coalesces to form film before the outbreak of spark formation in the ECDM process. A. Gok [17] has carried out a finite element simulation on chip formation while machining AISI 316H stainless steel. Turning tests were carried out at three different cutting speeds and constant depth of cut and feed rate. Predictions were compared with the orthogonal-cutting tests and found to agree. Further, A. Gok [18] investigated optimum cutting parameter values during turning of ductile iron using fuzzy TOPSIS and grey relational analysis. He has also developed an empirical model depending on cutting parameters of average surface roughness, maximum roughness, and main cutting force and feed force using response surface modelling. The adequacy of the developed model was proved by ANOVA and reported that the depth of cut was the dominant property on the surface roughness and cutting forces.

Gautam and Jain [19] proposed a valve theory based on the Finite Element Model (FEM) to demonstrate the discharge phenomenon in Electro-Chemical Spark Machining (ECSM) process. The proposed random location of the heat source to model the ECSM process. But they didn't made any simulation model to analyse the output responses. The MRR in ECDM was evaluated and modeled as a 3-D unsteady state heat conduction problem with the finite element method by Jain et al. [20]. Bhondwe et al. [21] modeled ECDM with FEM and reported that MRR got increased with duty factor, electrolyte concentration, and energy partition. They have not considerd the tool wear affecting the machining pocess. Panda et al. [22] have made FEM predict the MRR for various process parameters like duty factor, energy partition and have found that MRR increases with process parameters in Travelling Wire ECSM process. They have reported the need for taking sidespark in machining process. Jiang et al. [23] studied the energy of sparks experimentally to understand the electrochemical characteristics of tool electrodes. A FEM based model was proposed to correlate spark energy and the geometry of the removed material. The electrical energy

released by spark generation was transferred as thermal energy into the workpiece. The material removal due to chemical etching and thermal melting was taken in the study and have used tapered tool in experimental study. Predicted material removal by the model demonstrated a good correlation with experimental results. Chenjun et al. [24] modeled the ECDM process in the discharge regime with FEM and predicted the drilling depth in the discharge regime. Later they verified the model with experimental results. They have reported that almost 29% of power is transferred to the workpiece with pulsed DC power in machining. They have not considered the tool wear in the model.

Pravin P et al. [25] has conducted detailed study on the effect of machinng of borosilcate glass with various conventional and non conventional processes including Abrasive Jet Machining (AJM), Abrasive Water Jet Machining (AWJM), Laser machinng, Grinding and ECDM. They have concluded that ECDM process is widely used in borosilcate glass machinng due to its accuracy and cost effectiveness. R K Arya1 and A Dvivedi [26] has conducted experimental study on borosilcate glass machining. They have investigated the thermal stresses forming on borosilcate glass on ECDM machining and has optimised the parametrs for machining of glass with out fracture. Yang (2001) et al. had conducted experimental study on borolicate galss machining and has reported that chemical etching has major effect in machining amorphous structure. They have conducted experiment with various process parameters and have found that quality of the micro holes are improved with ECDM process. Kumar, S. and Dvivedi, A. [27] had used micro –Ultra Sonic Machining (USM) on borosilcate glass machining. They compared the experimental results with and without tool rotation and found that MRR is higher with 20% slurry with tool roation due to uniform distribution of abrasive particles between tool and workpiece. U. Aich et al. [28] studied the effect of water pressure, abrasive flow rate, traverse speed and standoff distance using Abrasive Water Jet Machining (AWJM) on borosilcate glass machining. They developed a model based on Particle Swam Optimisation (PSO) and reported that the depth of cut influences effect of process parameters in machining amorphous structure. H M Lee et al. [29] used femtosecond laser helical drilling method to machine different types of glasses including aluminium silicate glass, soda lime glass and borosilicate glass. They have reported higher MRR compared to other machining methods and found chemical composition affect the machining rate of glasses.

From the detailed literature review, most of the researchers concentrated on FEM model for sodalime glass and composites. Little work is concentrated on thermal modeling of the ECDM on borosilcate glass which has application micro fluidics, medical and fabrication industry. Also most of the researchers did not considered the side spark which also occurs in real time machining with ECDM. In the current work an attempt has been made to model and experimentally verify ECDM process on borosilcate glass. The industrial applications of borosilicate glass involve the production of pharmaceutical containers, fabricating slide, lenses and implantable medical devices. Due to its brittle and chemical inert nature, it is very difficult to machine with conventional machining methods. So the need a hybrid machining process such as ECDM is very relevant for making micro features in borosiclate glass. Curve fitting tool in MATLAB is used for finding the MRR obtained from the model. Tungston copper electrode is used as tool in current study to reduce the tool wear which will reduce the error percentage between experiemtal and modelled results. Also side spark taken in the modelling by selecting random numbers showing spark position, having values around the tool diameter. The main objective of the present work involves the thermal modeling of borosilicate micromachining with its experimental verification. The results are much promising for the borosilicate glass micromachining process. The discrepancies in the ANFIS and RSM model mentioned in the literature study are reduced to a greater extent in the current study. A FEM to predict the MRR in the discharge regime is discussed, and the model is experimentally verified in the present work. As an innovative developing hybrid machining process, ECDM modeling with experimental verification will contribute to further research in this process.

2 Modelling

The modeling approach of ECDM is demonstrated in Fig. 1. The finite element based model of ECDM is carried out under pulsed DC for MRR for multiple sparks (133), and results are validated. In the ECDM process, the continuous spark is responsible for the melting and vaporization of workpiece material resulting in MRR. In the model, it is pre-assumed that spark remains constant even though practically it varies with time. Chemical changes occurring in the electrolyte are neglected, and the spark temperature changes continuously in electrolyte near the workpiece, which is also pre-assumed to be constant.

2.1 Assumptions

The following are the assumptions that are made while modeling the ECDM process [21]:

1. Workpiece material is homogeneous and isotropic.
2. The energy of the spark is assumed to be identical.
3. Material removal takes place only because of thermal melting, and all the molten material is flushed away from the machining zone. Chemical etching is not considered.

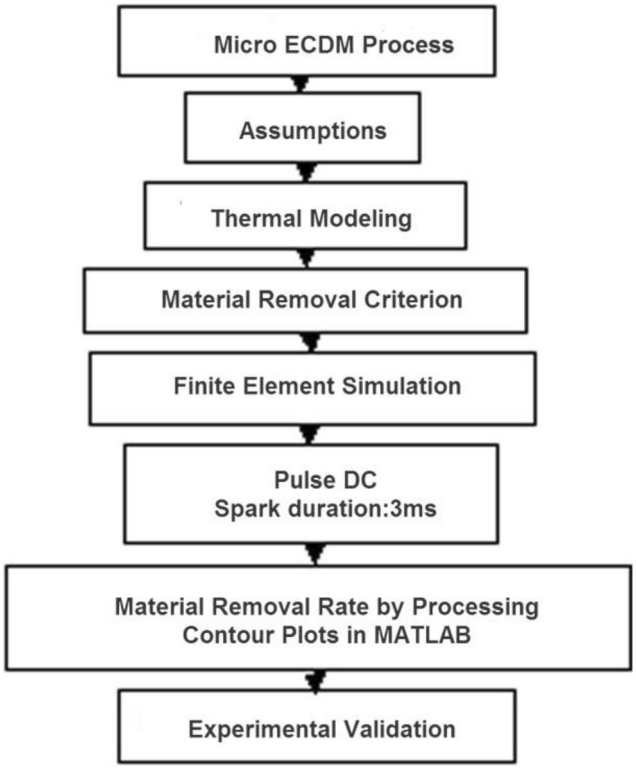

Fig. 1 Schematic Flow chart of FEM modelling in ECDM process

4. Only one spark at each discharge is considered for modeling
5. There is no heat loss due to convection along the sides of the domain since glass is a non-conductor
6. The spark occurs at a random position on the workpiece surface and is based on the shape of the tool; it is assumed that several sparks will occur near the axis of the tool.
7. The thermal expansion of the tool is not considered in this model [30].

Only thermal properties alone are used to find out the MRR and hence this can be considered as a heat conduction problem.

2.2 Thermal Modeling

Finite element modeling is carried out for a single spark, and the effect is studied with 133 sparks in the ECDM process. One hundred thirty-three sparks are selected to give significant magnitude for MRR in borosilicate glass, having a higher melting point. An axis-symmetric thermal model is developed to simulate the material removal process in the ECDM process. A rectangular portion with dimension 200×100 mm^2 is taken into account for 2D analysis. It is assumed that the material removal takes place only because of the sparks, which can be produced by melting and vaporization of the workpiece, and input is given in the form of heat flux. The spark has a circular cross-section and occurs at random locations on the surface of the tool. The important process parameters of MRR taken in the present model are critical voltage, partition energy and conductivity of the electrolyte. Critical current is calculated from the electrolyte conductivity since the current depends upon the conductivity of the electrolyte. These factors are used to find out the thermal heat flux that has to be supplied to the model. The governing equation for the present analysis is taken as given in Eq. (1) [24]:

$$k\left[\frac{1}{r}\left(r\frac{\partial T}{\partial r}\right)+\frac{\partial^2 T}{\partial z^2}\right]=\rho c\frac{\partial T}{\partial t} \tag{1}$$

where k, c, and ρ are the corresponding thermal conductivity, specific heat capacity, and density of the workpiece materials, respectively.

The preliminary condition is taken in such a way that the workpiece is kept inside the electrolyte, and the entire domain is assumed to have room temperature (t = 0), as shown in Fig. 2.

The boundary conditions applied includes

1. Boundary S_3 and S_4 are taken as insulated and $\frac{\partial T}{\partial n}=0$, where n indicates the normal direction to S_3 and S_4.
2. The heat transfer is assumed to be axis-symmetric about the spark axis so that heat flowing from and to counterpart is equal to the heat flowing to the counterpart. Therefore heat flowing across S_1 is zero. $\frac{\partial T}{\partial r}=0$, at r = 0.
3. On the surface S_2, where the spark occurs, heat flux boundary conditions are applied.

Based on the shape of the machined surface found [1], the heat source is represented as an exponentially decreasing function. Hence Gaussian heat flux expression [21] is used for this analysis. The Eq. (2): is given below.

$$q(r)=\frac{4.45\times Rw\times Vc\times Ic}{\pi\times R^2}e^{\left\{-4.5\times\left(\frac{r}{R}\right)^2\right\}} \tag{2}$$

Where,

R_w : Energy partition to the workpiece.

V_c : Critical voltage, volts.

I_c : Critical current, amps.

R : Radius of spark, μm.

r : Radial distance from the axis of the spark, μm

The thermal analysis for finding out the MRR during the ECDM process is carried out with PLANE 55 element in ANSYS-13 software, which meshes the rectangular region in the 2D analysis [4]. The properties of PLANE 55 elements with one Degree of Freedom (DOF) are suitable for this 2D heat conduction problem. The size of each meshed element is 10 μm, as obtained by mesh optimization shown in Fig. 3. During meshing, 20,000 elements and 20,300

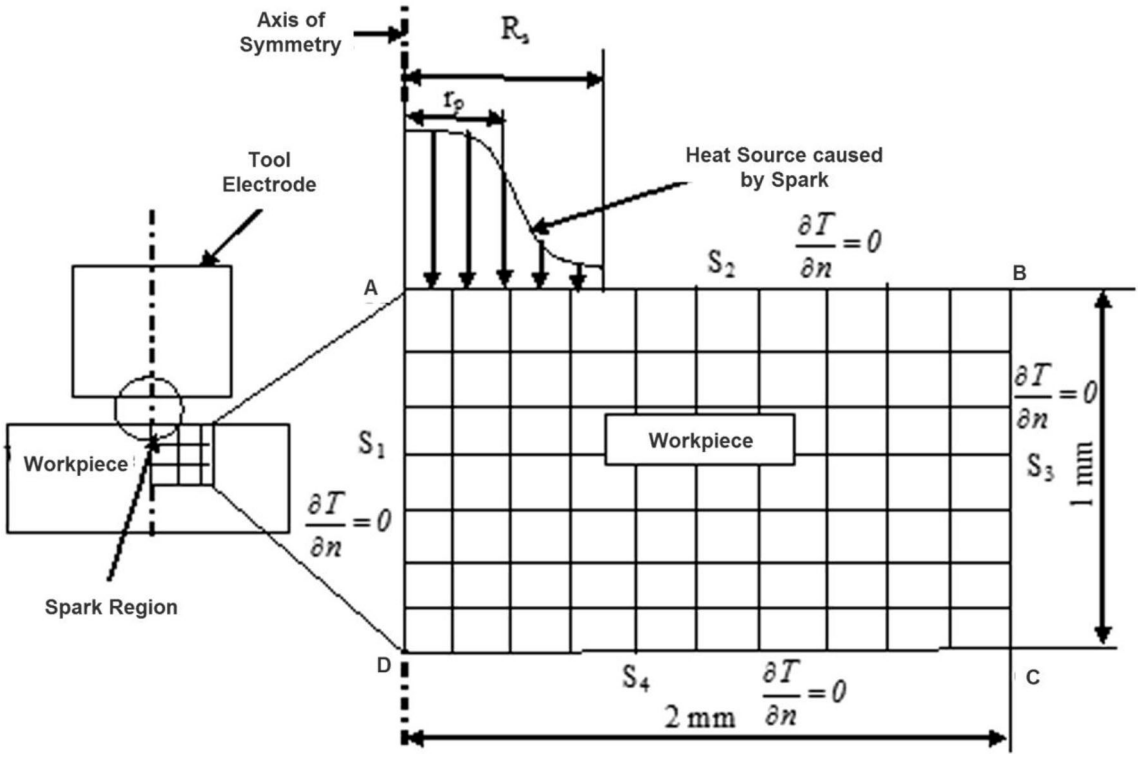

Fig. 2 ECDM thermal Model

nodes are generated. All known boundary conditions and loads are applied to the model to find out the desired output variables- temperature distribution. Since it is a time-dependent heat conduction problem, transient thermal analysis is selected for solving. At the start of this process, the workpiece is immersed in the electrolyte solution, and the temperature of the whole domain is taken as the room temperature of 305 K. Since borosilicate glass is a very poor conductor of heat, it is assumed that there is no heat loss due to convection on the top, bottom and the side domain surfaces of the workpiece. Thermal properties of borosilicate glass are given in Table 1. No heat transfer occurs along the axis-symmetric surface also. The heat flux is defined as a Gaussian distribution and is applied over the top surface of the workpiece [24].

The time of sparking is taken in pulsed DC as 3 ms/spark. Kulkarni et al. [1], has carried out machining on different engineering materials and have calculated the crater diameter to be 300 μm. So the radius of the spark is taken as 150 μm in the present study. In order to apply heat flux only within these 150 μm, a piece-wise continuous function as described in Eqs. (3): and (4): are used. By substituting the following values in Eqs. 2, 3 is obtained. In the present model, the partition energy is taken as 2%, but in the actual process, it might be more than 2% as most of the energy is assumed to be used for heating the electrolyte.

Critical Voltage, V_c : 40 V
Current, I_c : 0.14 amp
Partition Energy, R_w : 2%
Spark radius, r : 150 μm

$$q(x)=\begin{cases} 0, & D<0.00015 \\ 1.1946\times10^{8}\times\exp\left(-2\times10^{8}\times D^{2}\right), & -0.00015\le D\le 0.00015 \\ 0, & D>0.00015 \end{cases} \quad (3)$$

Where,

$$D = X - C1 \quad (4)$$

X : Coordinate of X-axis.
C_1 : Location of spark in the X-axis.

2.3 Material Removal Criterion

A table is created by using the above Gaussian heat flux function and using this table and heat flux are applied over the top surface of the tool. For of pulsed process, the spark occurs at

Table 1 Thermal properties of borosilicate glass

Properties	Values
Mass Density ρ, (kg/m^3)	2230
Melting Point(°C)	1093
Specific heat(J/kgK)	775
Thermal conductivity k(W/mK)	1.13

random locations on the bottom surface of the tool, and these locations are chosen by using the random numbers. Based on the shape of the machined surface, random numbers are chosen in such a manner that there will be a number of sparks near the axis of the tool. These random numbers are converted into locations of the spark C1. After defining the function and generating random locations, tables are defined using a unique name for each random location. Heat flux is defined over the top layer of the model using these tables. Based on the position of the spark (random location), heat flux will be applied on that surface. After applying heat flux at the first random location, the time of sparking is taken as 3 ms with ramped loading. These load data is stored in an LS (Load Step) file. The heat flux is applied gradually between the time intervals of 3 ms. This procedure is repeated for 133 times in order to achieve a total machining time of 399 ms. Then the model is solved by using these 133 LS files. All the results are viewed in the form of contour plots and graphs. The contour plot shows the temperature distribution at different nodes in the workpiece. Graph plots for temperature with time at different nodes can be obtained by using the time history post-processor option. The MRR is calculated by finding out the volume of materials having reached a temperature above its melting point (1094 K) [21]. By using the non-uniform contour plot, the region above its melting point is shown in a different colour. Then the best polynomial curve is selected using MATLAB tool by comparing it with the actual curve. A second-order polynomial is chosen for fitting since the shape of the machined region matches with this. By revolving this curve about the axis of the tool, the volume of material removed can be obtained.

The general equation for the second-order polynomial is given Eq. (5):

$$f(x) = \mathrm{p}_1\, \mathrm{x}^2 \;\; + \mathrm{p}_2 x + \mathrm{p}_3 \tag{5}$$

Where p_1,p_2, p_3 are constants.

By revolving this curve about the axis of the tool, Volume (V) of material removed is obtained as given in Eqs. (6) and (7):

$$V = -\int_0^{r_0} 2\pi x f(x)dx \tag{6}$$

substituting we get,

$$Volume = -2\pi\left[\frac{p_1 \times \mathrm{r}_0{}^4}{4} + \frac{p_2 \times \mathrm{r}_0{}^3}{3} + \frac{p_3 \times r_0{}^2}{2}\right] \tag{7}$$

where r_o is the intercept of the curve at the x-axis.

MRR is calculated by multiplying the volume rate of material removed with its density.

2.4 Pulsed DC Model

The modelling is performed for a 2D pulsed DC model with a total machining time of 399 ms with 133 sparks at different random locations. Mesh size is optimized as 10 μm. Figure 4 shows the temperature distribution across various nodes in the model. The maximum temperature obtained is 2316 K, and the minimum temperature obtained is 305 K (room temperature). It is observed that the maximum temperature occurs at a certain distance away from the axis of the tool. This is due to the fact that spark occurs at different locations and not concentrated at the centre of the tool. Figure 5 shows the amount of material removed by melting, followed by flushing during

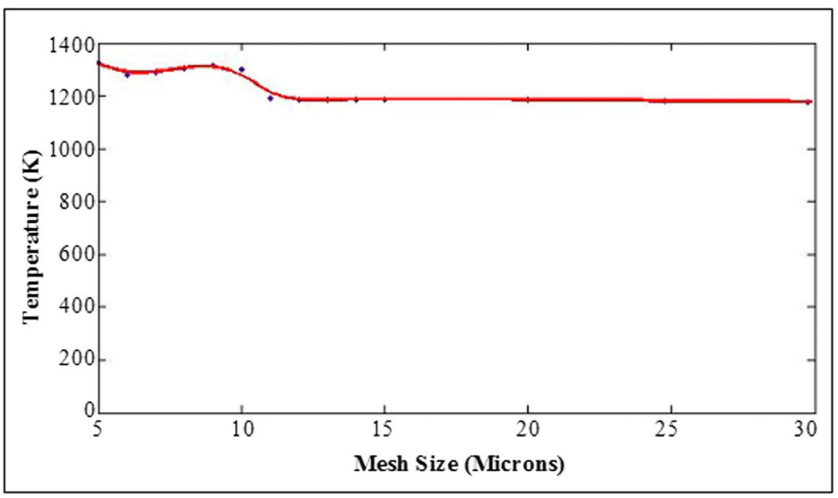

Fig. 3 Mesh Size optimisation

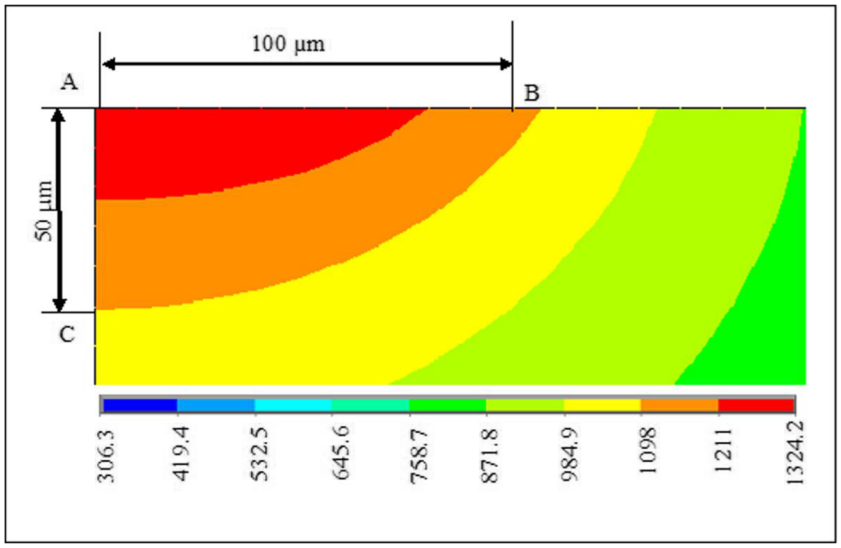

Fig. 4 FEM modelling on material removal rate

the ECDM process. The grey colour indicates the removed portion, and the red colour indicates the un-melted region. The width, r_0 of the removed region, is 108 µm, and the depth of the curve at the tool axis is 52.28 µm. MRR is calculated from the FEM model using a curve fitting in MATLAB. In order to model the curve, a quadratic polynomial equation is selected, as shown in Eq. (8):

$$f(x) = 0.005652\,x^2 - 0.1777x - 51.17 \tag{8}$$

From the above equation, the values of p_1, p_2,p_3 can be found out, and they are substituted in Eq. 6 to find out the volume of material removed as given in Eq.(9):

$$Volume = -2\pi\left[\frac{0.005652 \times 108^4}{4} + \frac{-0.1777 \times 108^3}{3} + \frac{-51.17 \times 108^2}{2}\right] \tag{9}$$

The MRR is calculated using the Eq. (10):

$$MRR = \frac{1.136 \times 10^6 \times 10^{-18} \times 2230 \times 10^6 \times 60}{399 \times 10^{-3}}\,\text{mg/min} \tag{10}$$

MRR =0.381 mg/min

The MRR in pulsed DC is due to the continuous breaking of the gas film formed in the pulsed circuit, which will result in electrolyte flow near the tool-workpiece interface. This will reduce the HAZ and lower the temperature in the case of pulsed DC. A graph between temperature and time at three different points on the model is shown in Fig. 6. The graph shows that there is a steep increase in temperature along the top surface of the workpiece, and it reduces gradually in-depth direction. The zigzag variation occurs due to the randomness of the spark locations on the top surface of the workpiece. The simulation results in Fig. 4 and Fig. 6 show the variation of

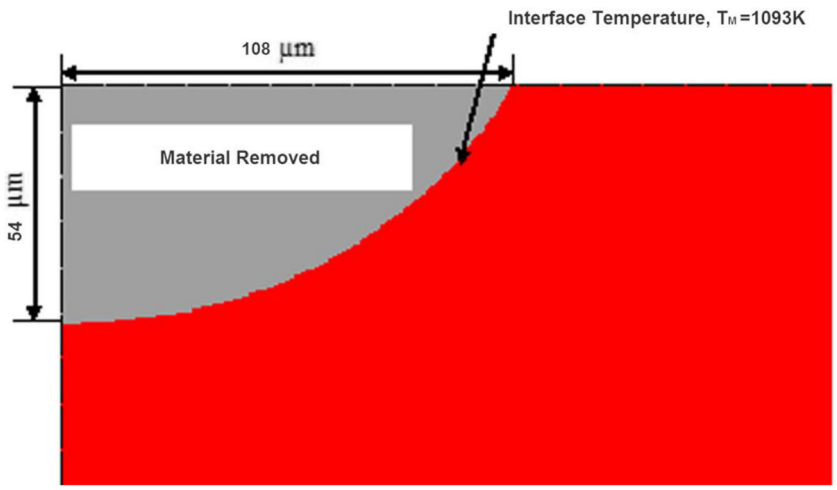

Fig. 5 FEM diagram of material removed

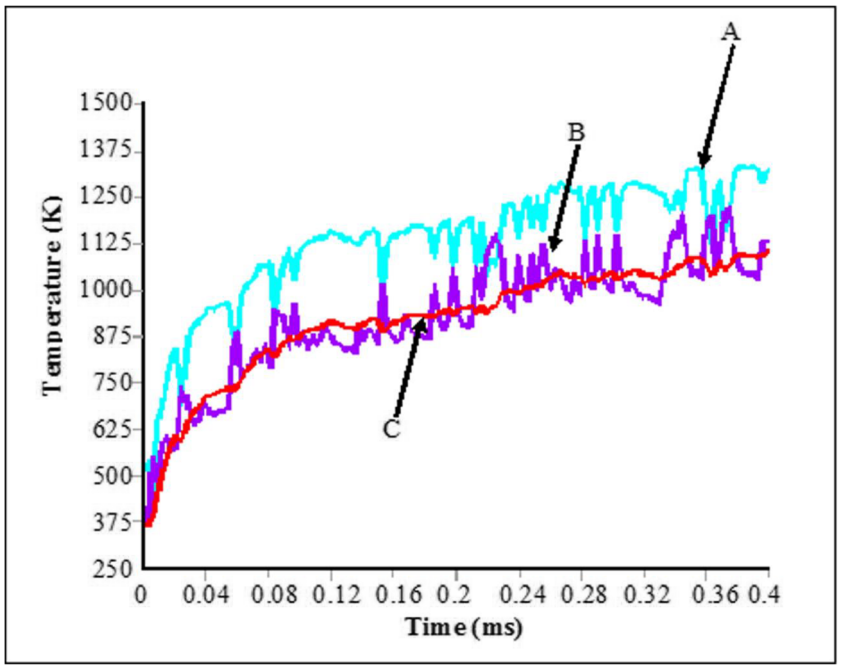

Fig. 6 Comparison of simulations of spark at different nodal position for 133 sparks

thermal energy at three spots, one on tool centre position and two others along with horizontal and vertical position in work-piece represented as A, B, C, respectively. The temperature at point A only reaches the melting point of glass resulting in material removal rate. The heat-affected region due to plastic deformation occurs in point B and C. Since glass has an amorphous structure, effect of chemical etching is also contributing in MRR which is considered only in experimental results, not in the simulation model.

3 Experimental Setups

The schematic setup of the ECDM process is represented in Fig. 7 and the experimental setup is given in Fig. 8. The setup includes the processing cell module and pulse generation module with a processing cell diameter of ∅200 mm. The electrode arrangement, work holding fixture, and tool holder are as shown in Fig. 8. The X-Y stage is assembled on to the portable aluminium breadboard table. The processing cell is

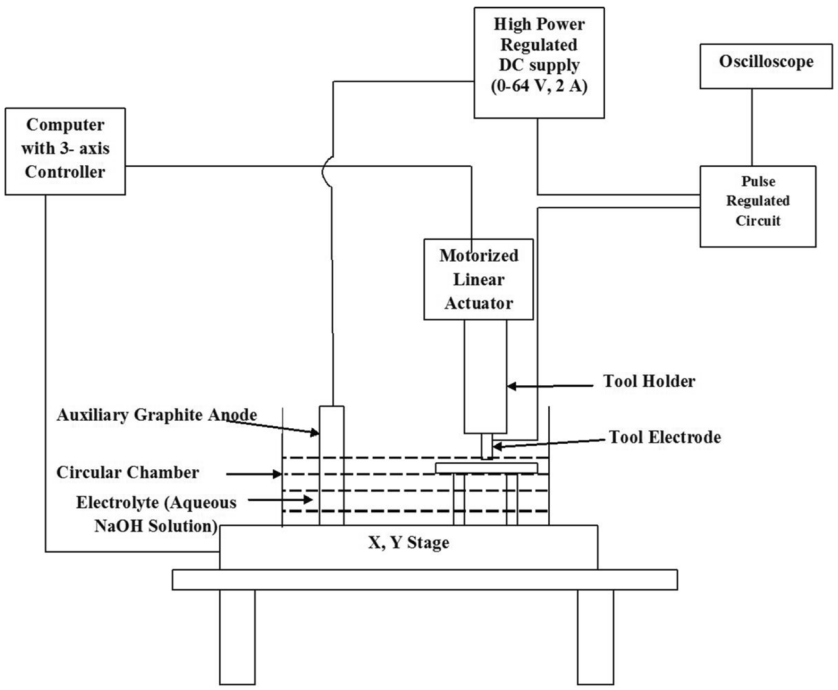

Fig. 7 Schematic Experimental setup

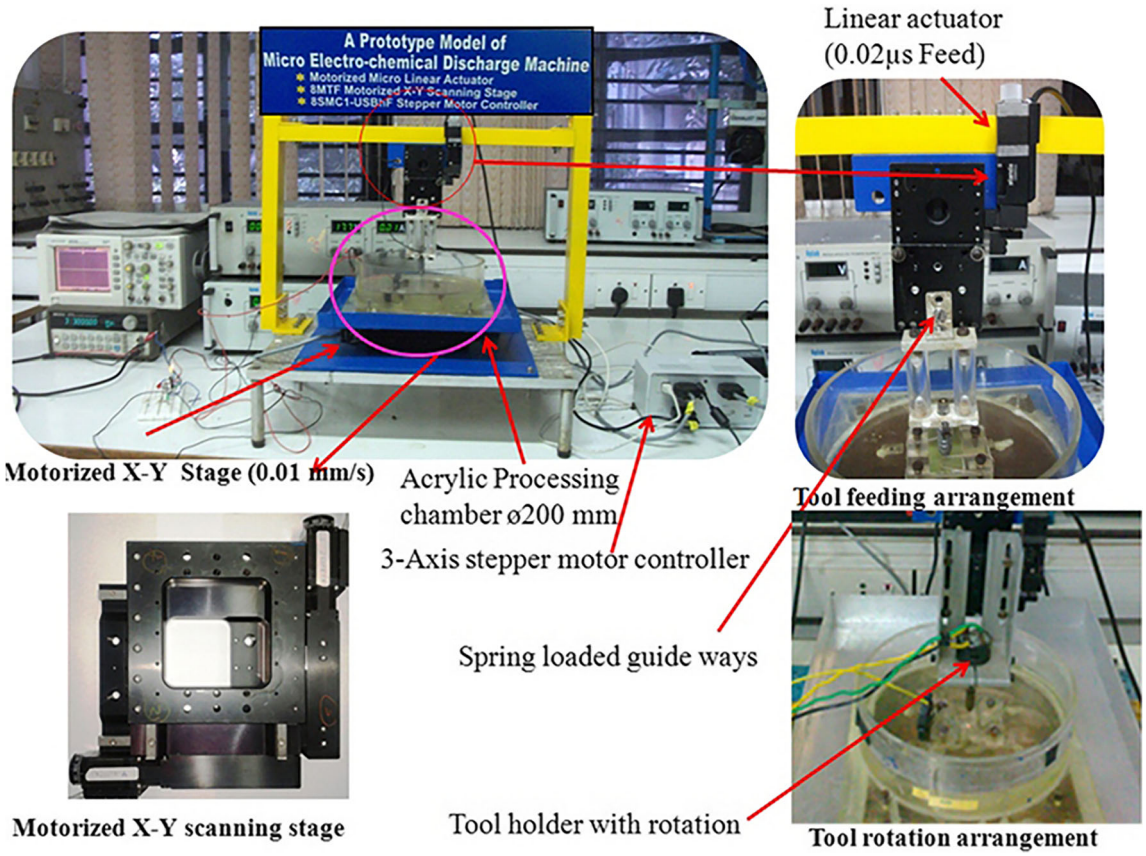

Fig. 8 Experimental setup

fixed over the X-Y stage. The linear actuator is attached to the spring-loaded guide ways and fixed to the horizontal aluminium rectangular cross-section tube. The Motorized X-Y Scanning Stage and Motorized Micro Linear Actuator are used for workpiece positioning and tool feeding during machining, respectively. Motorized X-Y Scanning Stage and Motorized Micro Linear Actuator with a resolution of 0.01 mm/s and 0.02 µs are used, with the help of a 3-axis stepper motor controller. Anode graphite plate had a surface area 100 times more than the tool surface and was kept in the electrolyte solution at 30 to 50 mm away from the cathode. The workpiece is mounted on the work table below the tool using a designed fixture and is dipped in the electrolytic solution at 2 to 3 mm below the electrolyte surface level.

3.1 Experimental Procedure

Sodium hydroxide electrolyte of known concentration is taken in the processing chamber. A graphite anode is placed at a distance of about 30 mm from the tool, which is a tungsten wire of 370 µm diameter. The borosilicate glass workpiece material is clamped over the work table, and the gap between the tool and workpiece is adjusted such that the tool is kept 1 mm above the workpiece. The properties of borosilicate glass are given in Table 1. The height of electrolyte is maintained between (2–3) mm above the workpiece surface, and a regulated DC power supply of (35–45) V is given to the electrolytic cell. It is noticed that when the voltage reaches 40 V, sparking starts at the tool-electrolyte interface. The process parameters are shown in Table 2. The further increase in the voltage causes the material removal due to melting and evaporation. The tool is fed at a controlled rate for one minute. The difference in the initial weight of the workpiece and the weight after machining gives the MRR (mg/min.). The experiments are conducted at different electrolyte concentrations, voltages, and duty factor with known time. The experimental validation is carried out based on 3 set of experiments. The repetitions are done to verify the error on measurement and experiment results are found to be satisfactory.

4 Experimental Validation of the Model

The predicted values are compared with the experimental results. The experimentally material removal rate (MRR) is found to be 0.414 mg/min with Grey Relation Analysis (GRA) [31] . An experiment is conducted using borosilicate glass as the workpiece material, tungsten wire as the tool, and sodium hydroxide (NaOH) as the electrolyte. The thickness of

Table 2 Process Parameters in ECDM Process

Item	Values
Workpiece material	Borosilicate glass
Elctrolyte	20,25,30 wt% NaOH
Applied voltage	25,40,45 V
Duty Factor	60,70,80
Tool electrode material	Anode: Graphite plate (30*20 mm^2), Cathode: Tungsten copper electrode
Machining time	7 min

the workpiece is 0.5 mm. The following are the optimized process parameters used while experimenting.

Critical Voltage, V_c : 40, volt

Critical current, I_c : 0.14, amp

Electrolyte Conductivity, c_e : 498 mS/cm

Time of machining, t : 7 min.

Electrolyte concentration : 30% by weight

Duty Factor : 70%

The value of MRR predicted by the model is 0.373 mg/min, and the experimentally obtained value is 0.414 mg/min. The percentage error is found to be 9.9%, which is within the permissible limits. The difference in MRR is due to recasting layer formation and lack of continuous spark during machining.

5 Results and Discussion

In ECDM, machining is due to the melting and vaporization of workpiece material by a spark. Also, 2–3% machining is due to chemical etching with electrolytes. In the FEM model, chemical etching is not considered. This is the main cause of the difference in MRR between the experimental value and modeled values. In experiments, the spark occurs randomly, and machining occurs due to side sparks occurring on the sides of the electrode also. This causes further melting and vaporization of the workpiece material. In FEM, the spark is assumed to occur more at the tool axis directions [24]. During the machining, some of the molten workpiece materials get solidified and get deposited back, which in turn reduces the MRR.

The main processing parameters are taken in experiment and voltage, electrolyte concentration, and duty factor, which are mentioned in Table 2, with its ranges. From the graph in Fig. 9, it is found that the chemical etching of glass increases with electrolyte concentration. Tungsten copper wire of diameter 370 μm used as a tool electrode and a graphite plate of 40 mm × 30 mm × 5 mm dimension is used as an auxiliary electrode. The effects of major processes parameters - concentration of an electrolyte, voltage, and duty factor on MRR are analyzed. Figure 9 shows the effect of electrolyte concentration on MRR while machining of borosilicate glass. The experiment is conducted for a fixed voltage of 40 V and a duty factor of 80%.

It is observed that the MRR increases gradually with an increase in electrolyte concentration due to chemical etching of the glass. With the increase of electrolyte concentration, the inter-electrode resistance between the tool and the auxiliary electrode decreases [8]. This increases the chemical etching on the workpiece surface. The spark intensity at the tool surface is high at 40 V and 80% duty factor. The heat produced on the workpiece surface accelerates the silicon dioxide present in the borosilicate glass to react with aqueous sodium hydroxide solution as follows:

$$2NaOH + SiO_2 \rightarrow Na_2SiO_3 + H_2O \quad (11)$$

The chemical etching rate increases with the concentration of the electrolyte. The quantity of (OH-) ions present in the electrolyte depends on the electrical conductivity of the electrolyte, which depends on the concentration of electrolyte. The (Na+) and (OH-) ions in the electrolyte are adsorbed by the glass surface. The (-Si-O-Si-) bond in a glass is broken and converted into the (-Si-O-Na-) bond during the chemical etching [32]. The (-Na-O-) bond formed is very weak compared to the siloxane bond (Si-O) present in the glass. The Na_2O-SiO_2 precipitate formed as a result of chemical etching is soluble in water due to its fragile (-Na-O-) bond present in the precipitate. This results in higher material removal due to chemical etching from the borosilicate glass surface. Low electrolyte concentration results in lack of etching and insignificant impact on MRR. Higher concentration results in irregular shaped micro features due to lack of control of process [21]. Also concentration of electrolyte beyond 30% resulted in uncontrolled etching resulting in irregular shapes [21].

Figure 10 shows the effect of voltage on MRR while machining of borosilicate glass. The experiment is conducted at a constant duty factor of 80% and a concentration of 25 wt%. It is observed that at lower applied voltage, the MRR is lower due to low spark intensity on the tool surface. When the voltage increases, spark intensity also increases. This will produce more heating effects on the tool-workpiece gap. Hence more material will melt and vaporize and results in high MRR

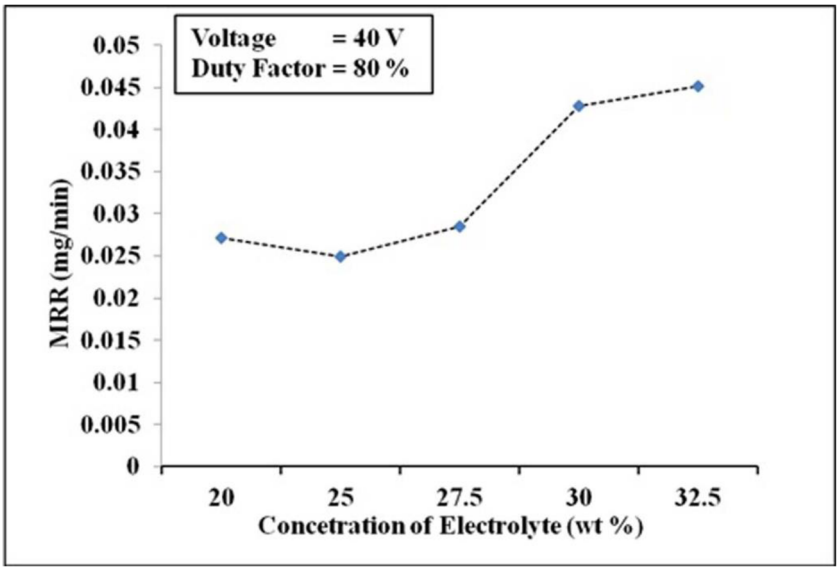

Fig. 9 Effect of Concentration on MRR

[33–35]. It is noted that at lower voltage (below 30 V) no spark is produced instead only hydrogen bubbles are produced and MRR obtained for the discharge voltage below 30 V was insignificant [21]. Also at higher voltage (above 45 V), spark is changed to arc and only surface heating is produced without any material removal [21].

Figure 11 shows the effect of duty factor on MRR while machining of borosilicate glass. The experiment is conducted at a constant voltage of 40 V and an electrolyte concentration of 25 wt%. The spark duration is increased with an increase in the duty factor. This increases the heat produced in the tool-workpiece gap, which accelerates the melting and vaporization of the glass workpiece [36]. At lower duty factor, the spark duration is reduced, which will cool the surface of the workpiece kept inside the electrolyte. This will reduce the HAZ formed on the glass surface. Similarly at lower duty factor, no spark is produced and has insignificant impact on MRR [22]. The duty factor above 80 resulted into large removal of workpiece with HAZ formation.

A simulation study has shown that material removal occurs in parabolic form, as mentioned in Figs. 4 and 5. In the simulation model, the axisymmetric shape of the hole is taken in assumptions, and so only half of the hole is shown in Fig. 5, which is in agreement with shape produced in the actual experimental condition in Fig. 12.

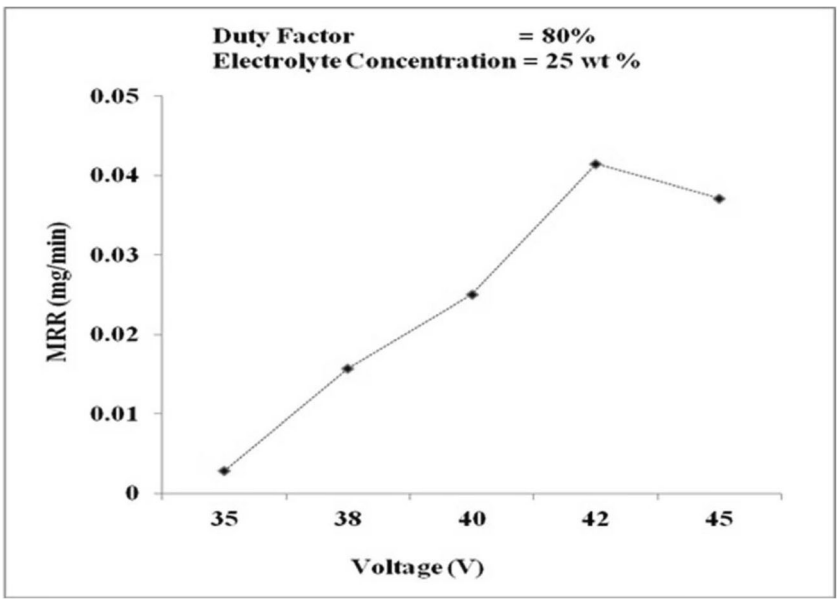

Fig. 10 Effect of Voltage on MRR

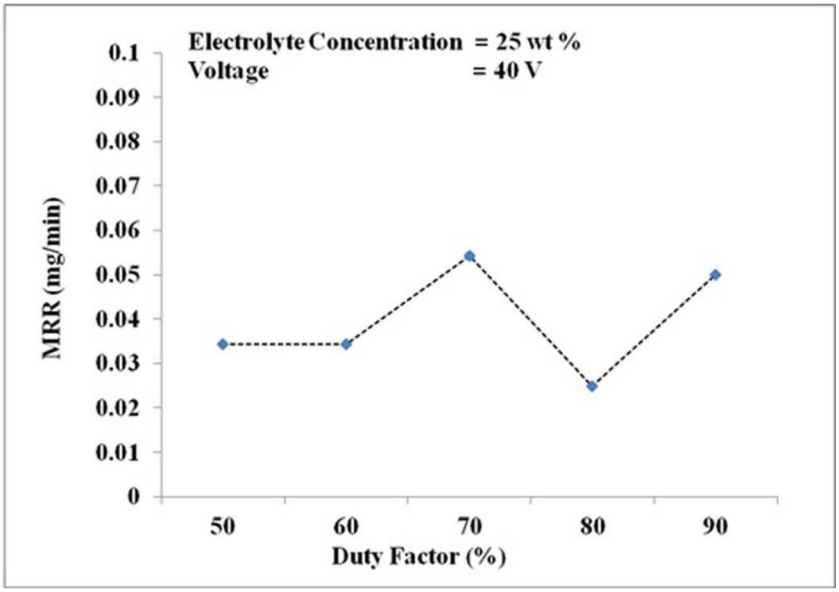

Fig. 11 Effect of Duty Factor on MRR

Bhondwe et al. [21] have mentioned the distribution of spark energy as a Gaussian distribution, which is taken in the current study. The craters and micro-holes produced in the current study are similar to those in the simulation model in Fig. 5. Also, the total energy from the spark is not fully used for machining as part of it is carried by electrolyte as convention [4]. So the transferring coefficient is taken as 0.2, which is one of the reasons for the lower value of MRR compared with the simulation model. Also, MRR produced is affected by the micro flow velocity of the electrolyte [21] and the heat transfer coefficient of liquid and gas phases. It has been reported that in machining with tapered tool [23], variation with the model was observed as tool wear was more. This limitation of tool wear is overcome in the current model with tungsten copper electrode having a higher melting point with a cylindrical cross-section. They have mentioned that the effect of chemical etching is predominant than a chemical reaction in the case of non-conducting materials like borosilicate in the present study. Also, the critical temperature below the melting point of the glass is essential for chemical etching.

The major applications of the current study include

- Proper selection of process parameter in borosilicate machining with ECDM process
- Proper selection of voltage for the ECDM process so as to reduce the power consumption
- Since the percentage of variation of MRR in simulation with respect experimental value is negligible, most of the assumption taken in the model can be taken as an accurate value

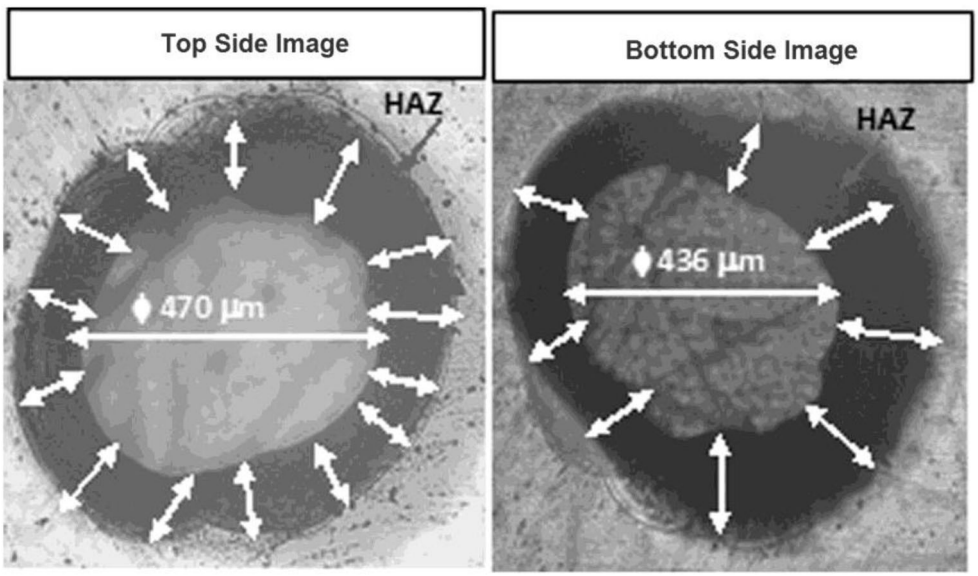

Fig. 12 Micro holes produced in Experiment

6 Conclusions

In the current paper, the Finite Element Model (FEM) of the ECDM process is made in the discharge regime with pulsed DC in the 2D domain to characterize MRR as a process response. MRR is calculated for multiple sparks in finite element modeling. The ECDM model gives a deeper insight into the process, which can be used for optimizing the process parameters of the process. The following conclusions are made from the finite modelling and experimental investigation carried out on the ECDM process.

- The MRR obtained for pulsed DC model it is 0.373 mg/min. The difference is very minute with the experimental value of 0.414 mg/min; hence it can be considered that there is almost negligible difference in MRR between experimental and model values with a 9.9% error variation.
- It is also found that the maximum temperature obtained in the pulsed DC process is 1316 K on a limited span of 108 μm.
- The variation in experimental results with modeled value is mainly due to chemical etching by electrolyte, which is not considered in the modeling. A factor for chemical etching in modelling will improve the result at par with experimental results.
- The range of parameters obtained from the experiments can be used for micromachining of borosilicate glass in various applications.

The future scope of the present work includes:

- The work can be extended to other asymmetric materials including quarts,semi conducting materials.
- A proper feedback system to monitor the process will improve the micro features produced in ECDM process.

Acknowledgments Not applicable

Financial Interests The authors declare they have no financial interests.

Author Contributions All authors contributed to the study conception and design. Material preparation, data collection and analysis were performed by Dr. Lijo Paul and Dr. Somshekhar SH. The first draft of the manuscript was written by Dr. Lijo Paul and all authors commented on previous versions of the manuscript. All authors read and approved the final manuscript. Authors are responsible for correctness of the statements provided in the manuscript.

Data Availability The data is trnaparent and available for publisher to publish in journal

Compliance with Ethical Standards

- The authors have no conflicts of interest
- No research involving Human Participants and/or Animals are conducted in current study

Conflicts of Interest/Competing Interests The authors have no conflicts of interest to declare that are relevant to the content of this article.

Consent to Participate Not applicable

Consent for Publication The authors have no conflicts of interest for publication of content of this article.

- The authors have no relevant financial or non-financial interests to disclose.
- The authors have no conflicts of interest to declare that are relevant to the content of this article.
- All authors certify that they have no affiliations with or involvement in any organization or entity with any financial interest or non-financial interest in the subject matter or materials discussed in this manuscript.
- The authors have no financial or proprietary interests in any material discussed in this article.
- Authors are responsible for correctness of the statements provided in the manuscript.

References

1. Kulkarni A, Sharan R, Lal GK (2002) An experimental study of discharge mechanism in electrochemical discharge machining. Int J Mach Tool Manu 42:1121–1127
2. Fascio V, Langen HH, Bleuler H, Comninellis C (2003) Investigations of the spark assisted chemical engraving. Electrochem Commun 5:203–207
3. Ali B, Mohammad RR (2016) Experimental study of the tool Wear during the electrochemical discharge machining (ECDM). Mater Manuf Process 31:574–580
4. Ali B, Mohammad RR (2016) Experimental and numerical study of material removal in electrochemical discharge machining (ECDM). Mater Manuf Process 31:495–503
5. Basak I, Ghosh A (1996) Mechanism of spark generation during electrochemical discharge machining: a theoretical model and experimental verification. J Mater Process Technol 62:46–53
6. Basak I, Ghosh A (1997) Mechanism of material removal in electrochemical discharge machining: a theoretical model and experimental verification. J Mater Process Technol 71:350–359
7. Wang W, Liu ZD, Tian ZJ, Huang YH, Liu ZX (2009) High efficiency slicing of low resistance silicon ingot by wire electrolytic-spark hybrid machining. J Mater Process Technol 209:3149–3155
8. Jui SK, Kamaraj AB, Sundaram MM (2013) High aspect ratio micromachining of glass by electrochemical discharge machining (ECDM). J Manuf Process 15:460–466
9. Pankaj KG, Akshay D, Pradeep K (2015) Effect of pulse duration on quality characteristics of blind hole drilled in glass by ECDM. Mater Manuf Process 31:1740–1748
10. Jinka R, Somashekhar SH, Lijo P (2011) Parametric analysis and a soft computing approach on material removal rate in electrochemical discharge machining. Int J Manuf Technol Manag 24:23–39
11. Roth HK, Wegener K (2013) Experimental investigation and simulation of heat flux into metallic surfaces due to single discharges in micro-electrochemical arc machining (micro-ECAM). Int J Adv Manuf Technol 68:1267–1275
12. Lijo P, Somashekhar SH, Jinka R (2014) Experimental investigation and parametric analysis of electro chemical discharge machining. Int J Manuf Technol Manag 28:57–79
13. Saranya S, Sankar AR (2018) Fabrication of precise micro-holes on quartz substrates with improved aspect ratio using the constant velocity feed drilling technique of an ECDM process. J Micromech Microeng 28(12):1–16

14. Nasim S, Mansour H, Mohammad RR (2018) Experimental study on the heat-affected zone of glass substrate machined by electrochemical discharge machining (ECDM) process. Int J Adv Manuf Technol 1:1–8
15. Mudimallana G, Apurbba KS (2017) On performance studies during micromachining of quartz glass using electrochemical discharge machining. J Mech Sci Technol 31(3):1365–1372
16. Tang W, Kang X, Zhao W (2019) Experimental investigation of gas evolution in electrochemical discharge machining process. Int J Electrochem Sci 14:970–984
17. Gok A (2017) 2D numeric simulation of serrated-Chip formation in orthogonal cutting of AISI316H stainless steel. Mater Technol 51(6):953–956
18. Gok A (2015) A new approach to minimization of the surface roughness and cutting force via fuzzy TOPSIS multi-objective grey design and RSA. Measurement 70:100–109
19. Gautam N, Jain VK (1997) Experimental investigations of ECSD process using various tool kinematics. Int J Mach Tool Manu 38: 15–27
20. Jain VK, Dixit PM, Pandey PM (1999) On the analysis of the electrochemical spark machining process. Int J Mach Tool Manu 39:165–186
21. Bhondwe VY, Kathiresan G (2006) Finite element prediction of material removal rate due to electro-chemical spark machining. Int J Mach Tool Manu 46:1699–1706
22. Panda MH, Yadava V (2009) Finite element prediction of material removal rate due to travelling wire electrochemical spark machining. Int J Adv Manuf Technol 45:506–520
23. Jiang B, Lan S, Ni ZJ (2014) Experimental investigation of spark generation in electrochemical discharge machining of non-conducting materials. J Mater Process Technol 214:892–898
24. Chenjun W, Kaizhou X, Jun N, Adam JB, Dejin H (2011) A finite element based model for electrochemical discharge machining in discharge regime. Int J Adv Manuf Technol 54:987–995
25. Pravin P, Raj B, Amaresh K (2017) Micromachining of borosilicate glass: a state of art review. Mater Today: Proc 4:2813–2821
26. Arya RK, Dvivedi A (2019) Thermal loading effect during machining of borosilicate glass using ECDM process. IOP Conf Series: Mater Sci Eng 647
27. Kumar S, Dvivedi A (2017) Experimental investigation on drilling of borosilicate glass using micro-USM with and without tool rotation: a comparative study. Int. J. AdditivSubtracte Mater Manufact 1:213–222
28. Ushasta A, Simul B, Asish B, Probal KD (2014) Abrasive water jet cutting of borosilicate glass. Procedia Mater Sci 6:775–785
29. Lee HM, Choi JH, Moon SJ (2020) Machining characteristics of glass substrates containing chemical components in femtosecond laser helical drilling. Int J of Precis Eng and Manuf-Green Tech: 1–11
30. Wuthrich R (2009) Micromachining using electrochemical discharge phenomenon: fundamentals and application of spark assisted chemical engraving. Elsevier Oxford, UK
31. Lijo P, Somashekhar SH (2014) Evaluation of process parameters of ECDM using Grey relational analysis. Procedia Mater Sci 5: 2273–2282
32. Mochmaru Y, Ota M, Yamaguchi K (2012) Micro hole processing using electro-chemical discharge machining. J Adv Mechan Design, Syst Manufact 6:949–957
33. Didar TF, Dolatabadi A, Wuthrich R (2008) Characterization and modeling of 2D-glass micro-machining by spark-assisted chemical engraving (SACE) with constant velocity. J Micromechan Micro Eng 18:1–10
34. Lijo P (2015) Characterization of micro features produced using μ-ECDM process: experimental and theoretical investigations. A dissertation submitted to IIT Madras, Chennai
35. Singh M, Singh S, Kumar S (2020) Experimental investigation for generation of micro-holes on silicon wafer using electrochemical discharge machining process. Silicon 12:1683–1689
36. Yang CT, Ho SS, Yan BH (2001) Micro hole machining of borosilicate glass through electrochemical discharge machining (ECDM). Key Eng Mater 196:149–166